*Nordic Hydrology* (1971), II, 1–22
Published by Munksgaard, Copenhagen, Denmark


# NUMERICAL ANALYSIS OF FINITE DEPTH PROBLEMS IN SOIL-WATER HYDROLOGY

K. K. WATSON

School of Civil Engineering, The University of New South Wales, Kensington, Australia.

The types of initial and boundary conditions which may be involved in the flow of water through an unsaturated profile to a water table are discussed. A numerical solution of the flow equation is then outlined and its use in the one-dimensional drainage of a homogeneous profile and in ponded infiltration into a draining profile detailed. Several characteristics of the drainage of deep profiles are discussed together with numerical solutions for the drainage of a stratified profile and infiltration into a draining profile.

In this paper soil-water hydrology refers to that part of the hydrologic cycle concerned with the movement of water in the unsaturated zone. This zone is defined at its upper boundary by the soil surface and at its lower boundary by the water table. The analysis of the hydrologic processes involved can become exceedingly complex when factors such as intermittency of surface flux with time, heterogeneity of the soil profile, root extraction, and thermal and chemical gradients are included. If the water table is at great depth, it is usual to consider the problem in terms of an infinitely deep profile and, accordingly, no hydraulic continuity between the water table and the soil surface is assumed. However, if the depth to water table is such that a usable solution requires consideration of the entire profile, the problem must be analysed as one of finite depth with a lower boundary condition of zero pressure head (relative to atmospheric pressure). This paper is primarily concerned with finite depth solutions.

A valuable conceptual framework of water movement in unsaturated soils has been developed using quasi-analytical methods. A summary of this work, particularly in regard to the theory of infiltration, has recently been given by Philip (1969). Although such studies are particularly instructive and allow general statements to be made concerning the physics of the phenomena, they suffer the disadvantage of being restrictive concerning initial and boundary conditions and the medium properties. Such restrictions eliminate from precise analysis a wide range of problems which simulate field conditions. However, these problems become quite tractable when the differential flow equations are solved by finite difference methods using a high speed digital computer. This approach is ideal in providing solutions for a particular porous material and specified initial and boundary conditions. If more general statements are required, it is necessary to obtain a broad range of numerical solutions so that a comprehensive description of the physical system can be given.

The simplest finite depth problem is the one-dimensional gravity drainage of an initially saturated homogeneous profile to a stationary water table. This has received attention from several investigators including Liakopoulos (1964), Watson (1967), Jensen & Hanks (1967), and Whisler & Watson (1968). The numerical method will be illustrated by reference to this problem and the drainage characteristics of deep profiles will be discussed in the light of the computer solutions. The system can be extended by considering the drainage of the profile to a falling water table. This has particular relevance in studying delayed yield effects in pumping tests in unconfined aquifers.

In the analysis of certain groundwater recharge operations the drainage of the saturated profile forms a suitable initial condition prior to the establishment of some intermittent pattern of water application to the surface. Upon rewetting, the boundary draining relationship between water content and pressure head is no longer applicable and the primary hysteresis scanning curves must be used. Whisler & Watson (1969) have analysed ponded infiltration into a draining profile and some characteristics of this analysis will be discussed later in this paper. In cases where ponding does not occur (e. g. sprinkler irrigation) infiltration will proceed at rates less than infiltration capacity.

The next phase in the cycle of intermittent recharge occurs when the ponded infiltration is terminated. Redistribution of the infiltrated water then occurs often while the lower section of the profile is continuing to drain. This problem has also been analysed by Watson & Whisler but is awaiting experimental confirmation prior to publication.

The above pattern of wetting and redistribution can be repeated either regularly or randomly in time. The degree of complexity involved in the analysis will depend principally on the timing of the events. This may vary from a suc-

cession of input pulses of water at one extreme to such long intervals at the other that wetting-up will follow the boundary wetting curve. As the history of wetting and draining becomes more complicated, the handling of the hysteresis information becomes more formidable. In addition, superimposed on this gravity field condition will be the movement of water from the soil in an upward direction due to evaporation or evapotranspiration.

Under certain circumstances the ponding of water on the soil surface can result in changes in the pore air pressure between the descending wet front and the lower profile. This effect can be included in the flow equation but as yet little has been documented for such a system.

It is rare to find soil profiles that are homogeneous. The lack of homogeneity can be classified for our purposes into layered systems and those which are generally heterogeneous in one dimension. In considering the vertical drainage of layered systems there is no difficulty in analysing a system where a coarser layer overlies a finer layer. An example of such an analysis is provided later in this paper. However, where a finer layer overlies a coarser layer the drainage of the lower layer becomes more complex due to limited air access across the interface. As yet a detailed analysis of this system has not apppeared in the literature. Where a profile exhibits general one-dimensional heterogeneity, $K(\Theta)$ and $h(\Theta)$ will vary with depth.

In the above discussion only one-dimensional flow has been considered. However, most of the statements made are applicable to flow in more than one dimension.

Recent experimental work (Sedgley 1967) has suggested that, at least during drainage, the moisture characteristic determined by dynamic means is different from that obtained using equilibrium methods. Additional work is required on this aspect, which, if fully proven, would indicate that a moisture characteristic dependent on the flow process itself would be necessary.

## NUMERICAL ANALYSIS

The form of the flow equation most suitable to the analysis of finite depth problems of the type discussed above is the pressure head form. For vertical isothermal flow in a homogeneous porous material this may be represented as:

$$C(h)\frac{\partial h}{\partial t} \equiv \frac{\partial}{\partial z}\left(K(h)\frac{\partial h}{\partial z}\right) + \frac{\partial K(h)}{\partial z} \qquad (1)$$

where $h$ is the pressure head of water in the porous material measured in cm of water (negative for unsaturated conditions), $t$ is the time from the start of drainage, and $z$ is the depth below the surface defined as positive in the upward direction and measured in cm. The volumetric water capacity is $C(h) \equiv \frac{d\Theta}{dh}$ where $\Theta$ is the volumetric water content in cm³ of water/cm³ of porous material. $K(h)$ is the hydraulic conductivity of the material in cm/min as a function of pressure head, although in the data input it is presented in terms of $K$-$\Theta$.

In this section the numerical procedure will be illustrated by reference firstly to the drainage of an initially saturated column and secondly to ponded infiltration into a draining column. The numerical analysis has been previously detailed by Whisler & Watson (1968) but will be repeated here for convenience.

**Drainage of Homogeneous Saturated Profile to a Water Table**

The boundary conditions for this system are as follows:

Upper boundary:

$$-K(h)\left(\frac{\partial h}{\partial z}+1\right)_{z \equiv o} = 0 \qquad t>0 \tag{2}$$

Lower boundary:

$$h(z,t)_{z=-L} \equiv 0 \qquad t>0 \tag{3}$$

where $L$ is the length of the column.

These equations express respectively the zero flux condition across the upper surface and the presence of the water table. The initial condition can be written in a general form as:

$$h(z,0) = h_o(z) \qquad -L<z<0 \tag{4}$$

where $h_o(z)$ is some distribution of the pressure head in the column. If hysteresis effects are to be neglected, it is sufficient to state that $h_o(z)$ is chosen so that all points in the column would drain for $t>0$. Since, for the sands considered, the $\Theta(h)$ relationship exhibited a very definite air entry value, the form of the initial pressure head distribution was assumed to vary linearly from zero at the water table to the air entry value at the soil surface. This approach saves considerable computer time and generally is assumed physically correct although recent experimental studies have indicated that the linear pressure profile as specified does not occur instantaneously on the movement of the water films through the surface grains.

To solve Eq. (1) numerically, a grid of points was superimposed on the region $t \geq 0$, $-L \leq z \leq 0$. The $z$ axis was divided into $N$ intervals ($N \equiv 100$). The mesh points are defined by:

$$t_m \equiv m \triangle t \quad m \equiv 0, 1, 2 \ldots \tag{5}$$

$$z_n \equiv -(N - n + 1) \triangle z \qquad n \equiv 1, 2 \ldots N + 1 \tag{6}$$

$$\triangle z = L/N \tag{7}$$

The partial derivatives in (1) were approximated by the finite differences:

$$\frac{\partial}{\partial z}\left[K(h)\frac{\partial h}{\partial z}\right] \approx \frac{1}{2(\triangle z)^2}\left[K_{n+1/2,m-1/2}(h_{n+1,m} + h_{n+1,m-1} - h_{n,m} - h_{n,m-1})\right.$$

$$\left. - K_{n-1/2,m-1/2}(h_{n,m} + h_{n,m-1} - h_{n-1,m} - h_{n-1,m-1})\right] \tag{8}$$

$$\frac{\partial h}{\partial t} \approx \frac{h_{n,m} - h_{n,m-1}}{\triangle t} \tag{9}$$

$$\frac{\partial K(h)}{\partial z} \approx \frac{K_{n+1/2,m-1/2} - K_{n-1/2,m-1/2}}{\triangle z} \tag{10}$$

where arbitrarily

$$K_{n+1/2,m-1/2} = \frac{K_{n,m-1} + K_{n+1,m-1} + K_{n+1,m} + K_{n,m}}{4} \tag{11}$$

and a similar definition is true for $K_{n-1/2,m-1/2}$

The finite difference approximations (8) through (11) were substituted into Eq. (1) to obtain a set of $N - 3$ algebraic equations of the form:

$$E_n h_{n-1,m} - F_n h_{n,m} + G_n h_{n+1,m} = -H_n \tag{12}$$

where

$$E_n = K_{n-1/2,m-1/2} \tag{13}$$

$$F_n = \frac{2C_{n,m-1/2}}{r} + E_n + G_n \tag{14}$$

$$G_n = K_{n+1/2,m-1/2} \tag{15}$$

$$H_n = G_n(h_{n+1,m-1} - h_{n,m-1}) - E_n(h_{n,m-1} - h_{n-1,m-1}) \tag{16}$$

$$+ 2\triangle z(G_n - E_n) + 2C_{n,m-1/2}\frac{h_{n,m-1}}{r}$$

where

$$C_{n,m-1/2} = \frac{C_{n,m-1} + C_{n,m}}{2} \tag{17}$$

and

$$r \equiv \frac{\triangle t}{(\triangle z)^2} \tag{18}$$

When Eq. (12) is applied at $n=2$ and the boundary condition (3) is invoked, the result is:

$$-F_2 h_{2,m} + G_2 h_{3,m} = H_2 \tag{19}$$

At $n=N$ with boundary condition (2) being invoked, the result is:

$$E_N h_{N-1,m} - (F_N - G_N) h_{N,m} \equiv - (H_N - G_N \triangle z) \tag{20}$$

Eqs. (12), (19), and (20) constitute a set of $N-1$ algebraic equations in $N-1$ unknowns. Since the coefficients $E_n$, $F_n$, $G_n$, and $H_n$ in these equations depend on values of $h_{n,m}$, they are nonlinear algebraic equations. This nonlinearity was satisfactorily handled using an iterative process. The steps in the solution are as follows:

*(A)* The initial condition was used to give the first set of $h_{n,m-1}$ values.

*(B)* This condition was also used to give the first estimate of $h_{n,m}$ values for the purposes of estimating the coefficients $E_n$, $F_n$, $G_n$, and $H_n$.

*(C)* The resulting set of linear algebraic equations was solved by an algorithm for an improved estimate of $h_{n,m}$ values.

*(D)* The improved estimate of $h_{n,m}$ was in turn used to get new values of $E_n$, $F_n$, $G_n$, and $H_n$, giving a second improved estimate, etc.

*(E)* The results of each iteration were compared with those of the previous iteration and when satisfactory convergence was reached (say $\pm$ 0.01 cm), the last estimate of $h_{n,m}$ values was retained and considered to apply at $t_m \equiv \triangle t + t_{m-1}$.

*(F)* The iteration was then repeated for successive time steps (see *(H)* below) to build up the time and space dependence of $h$.

*(G)* At the end of each time step the pressure head at the top of the column $h_{N+1}$ was calculated from

$$h_{N+1} \equiv h_N - \triangle z \tag{21}$$

*(H)* Rather than use tabular $\triangle t$ values, an initial small value was used (say $10^{-6}$ min) and at the end of each time step the following tests were made,

$$(h_{n,m} - h_{n,m-1}) \gtrless \delta_1 \tag{22}$$

and

$$(h_{n,m} - h_{n,m-1}) \gtrless \delta_2 \tag{23}$$

where

$$\delta_1 > \delta_2$$

If the first test was greater than $\delta_1$, then $\triangle t_{\text{new}}$ was set equal to (3/4) $\triangle t_{\text{old}}$ and the time step was repeated. If the first test was less than $\delta_1$ and the second test greater than $\delta_2$, $\triangle t$ remained the same. If the first test was less than $\delta_1$ and the second test less than $\delta_2$ for all points, then $\triangle t_{\text{new}} = 2\triangle t_{\text{old}}$ and the next step was calculated. This allows automatic programming of $\triangle t$ although the actual numerical values emerge as part of the solution.

*(I)* The cumulative outflow from the column was calculated by numerically integrating:

$$Q \equiv \int_{-L}^{o} \Theta(h,t)dz - \int_{-L}^{o} \Theta(h,0)dz \tag{24}$$

This equation gives $Q$ negative in sign for drainage.

**Ponded Infiltration into a Draining Profile**

In such a system infiltration is occurring at the top of the profile while drainage is continuing in the lower part of the profile. The possibility of pore air pressure changes in the zone between the draining and wetting fronts is neglected in this analysis. Whisler & Watson (1969) have discussed such a system.

The boundary conditions for the system are:

Upper boundary: $h(z,t)_{z=o} = h_T \qquad t > 0$ (25)

Lower boundary: $h(z,t)_{z=-L} = 0 \qquad t > 0$ (26)

where $h_T$ is the depth of the ponded water during inundation.

The initial condition is

$$h(z,t) \equiv h(z) \qquad t \equiv t_o, \qquad 0 \geq z \geq -L \tag{27}$$

This initial condition could be the linear equilibrium pressure profile or a nonsteady-state drainage profile at an intermediate time calculated by the method already given.

The finite difference method discussed previously is equally applicable to this system. The main difference between the procedures is the necessity in the ponded case to allow for wetting up along the scanning curves. The method used to take this hysteresis effect into account is based on the flux of water at a point.

The flux of water into and out of each point $n$ is

$$F_{\text{in}} = -K_{n+1/2,m-1}\left(\frac{h_{n+1,m-1}-h_{n,m-1}}{\Delta z}+1\right) \tag{28}$$

$$F_{\text{out}} = -K_{n-1/2,m-1}\left(\frac{h_{n,m-1}-h_{n-1,m-1}}{\Delta z}+1\right) \tag{29}$$

If $F_{\text{in}}<F_{\text{out}}$, drainage relationships of $K(h)$, $C(h)$, and $\Theta(h)$ are used.

If $F_{\text{in}}>F_{\text{out}}$, the following procedure is carried out:

*(A)* A column matrix called $U$ equal in size to the number of position indices is set up initially with all $U_n \equiv 0$.

*(B)* While drainage is occurring, $U_n$ is unchanged.

*(C)* When wetting is first indicated, $U_n$ is set equal to $h_{n,m-1}$ and kept at that value for the remainder of the run.

*(D)* $U_n$ is used to identify that point for looking up the appropriate wetting scanning curve in the $K(h)$, $C(h)$, $\Theta(h)$ tables.

*(E)* Each scanning curve is identified by the value of the pressure head where it departs from the draining curve. For scanning curves intermediate to the tabular set of scanning curves, linear interpolation is used.

## COMPUTED RESULTS

### Vertical Drainage of Homogeneous Profiles

Two sands were used in this study, Botany sand and G1 sand. Both sands are fairly uniform in grading, the former having an air entry value, after slight rounding of the $h(\Theta)$ curve at that point, of –38 cm and the latter –29 cm. The $h(\Theta)$ and $K(\Theta)$ relationships of the two sands are given in Figures 1 and 2.

Although in this study we are particularly interested in the drainage charac-

teristics of deep profiles, a wide range of profile depths has been considered. These depths were 60, 80, 100, 120, 150, 180, 250, 300, 500, 600, and 800 cm for the Botany sand and 120, 300, and 800 cm for the G1 sand.

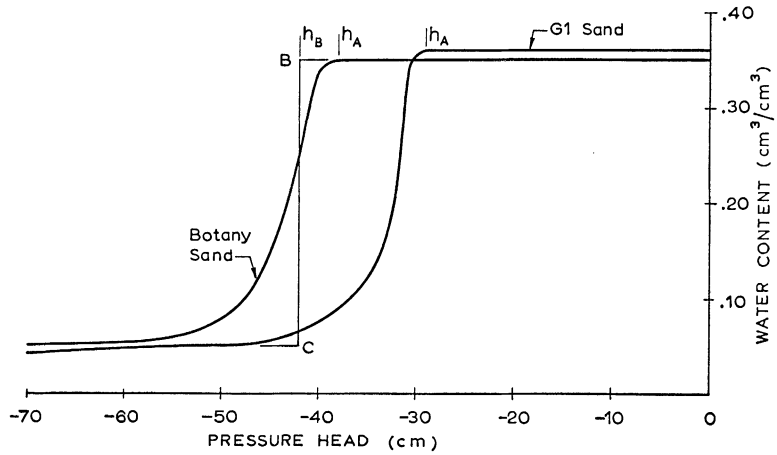


*Fig. 1.*
Pressure head–water content relationship for Botany sand and G1 sand.

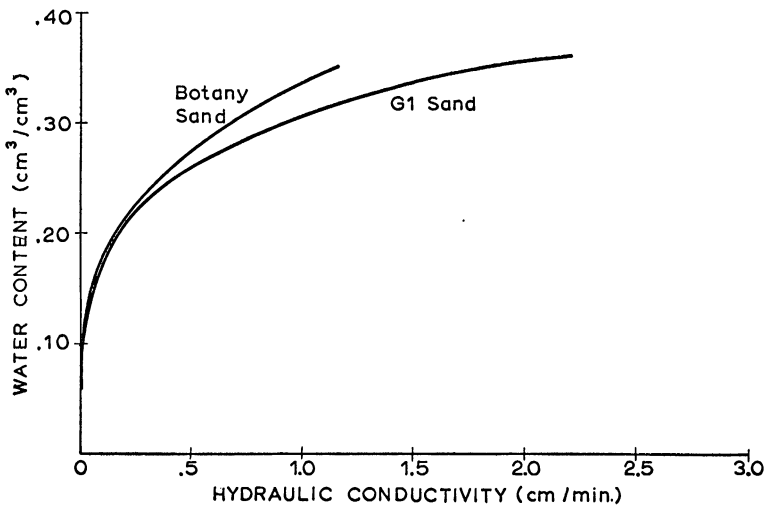


*Fig. 2.*
Hydraulic conductivity–water content relationships for Botany sand and G1 sand.

Figure 3 gives $h(z, t)$ for a 120 cm depth of Botany sand. Figure 4 gives the corresponding $\Theta(z, t)$ relationship. The initial pressure head condition is a linear one varying from zero at the water table to the air entry value (–38 cm) at the surface. The characteristic shape of the pressure profiles as drainage continues may be noted from Figure 3, particularly the form as equilibrium is approached. Although the profile at 2.49 days is adjacent to the equilibrium profile, equilibrium was not reached until 8.19 days, the slow pressure change being due to the very small conductivity values in the pressure head range –80 cm to –120 cm.

$h(z, t)$ and $\Theta(z, t)$ for a 800 cm column of Botany sand are given in Figures 5 and 6 respectively. The $h(z, t)$ curves have zones where the pressure head changes are very small. Figure 5 shows clearly the practical impossibility of a profile of this depth draining to equilibrium. Although the pressure head differences between the 17 day pressure profile and equilibrium are very large, the

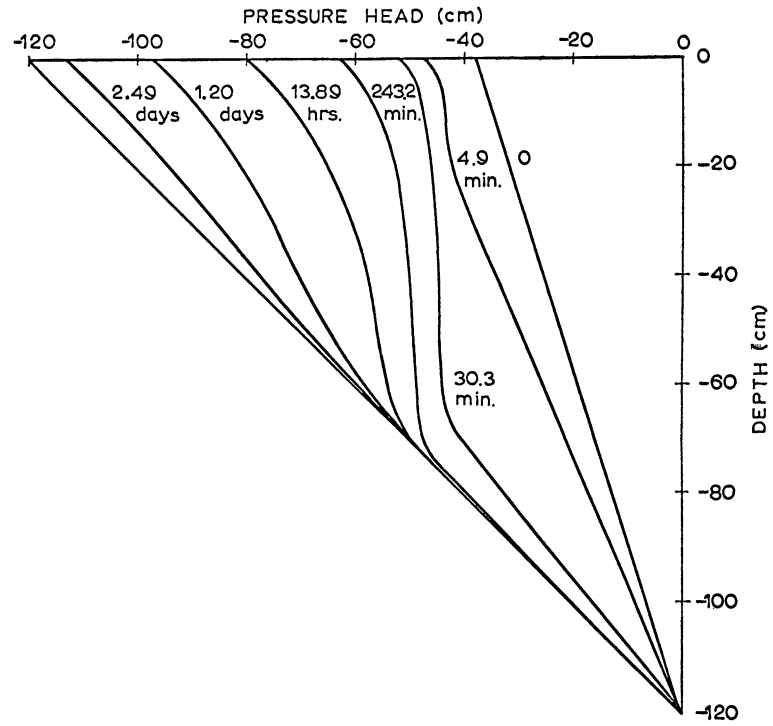


*Fig. 3*
Pressure head profiles for a 120 cm depth of Botany sand.

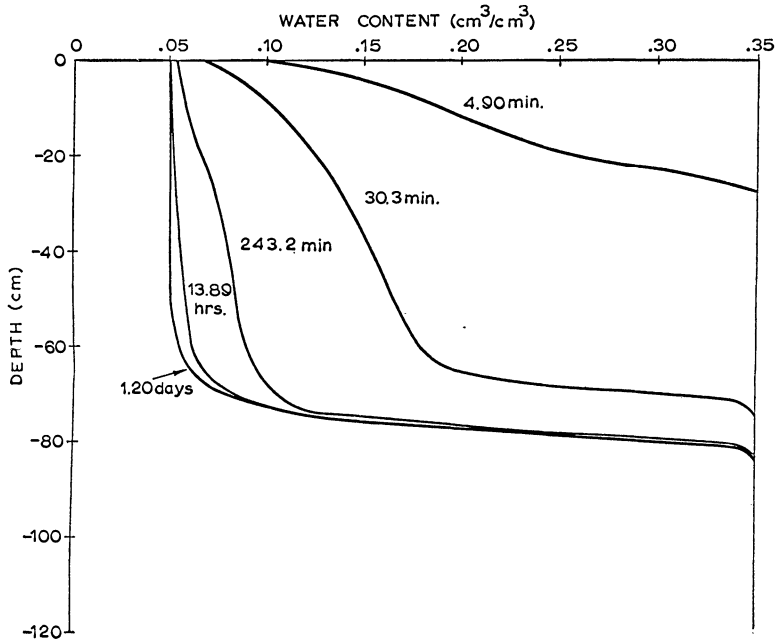


*Fig. 4.*
Water content profiles for a 120 cm depth of Botany sand.

volume of water still to drain is small due to the almost horizontal form of $h(\Theta)$ at these pressure heads. This fact may be noted by reference to Figure 6.

The availability of numerical solutions not only provides a ready means of analysing deep profiles but also provides a convenient way of finding the time to reach equilibrium for different depths of profile. Figure 7 gives this relationship for Botany sand for depths up to 150 cm. For this depth the numerical estimate is 23.1 days to attain equilibrium. The relationship begins to flatten considerably in the vicinity of this depth, indicating that for depths to any extent greater than this equilibrium will not occur.

Figure 8 illustrates the time required to reach certain values of $Q/Q_\infty$ for different depths. Here $Q$ is the total outflow at the time in question and $Q_\infty$ is the total outflow for equilibrium conditions. For values of $Q/Q_\infty$ of .90 .95, and .97, the relationships are linear but at the higher $Q/Q_\infty$ values they become slightly curved.

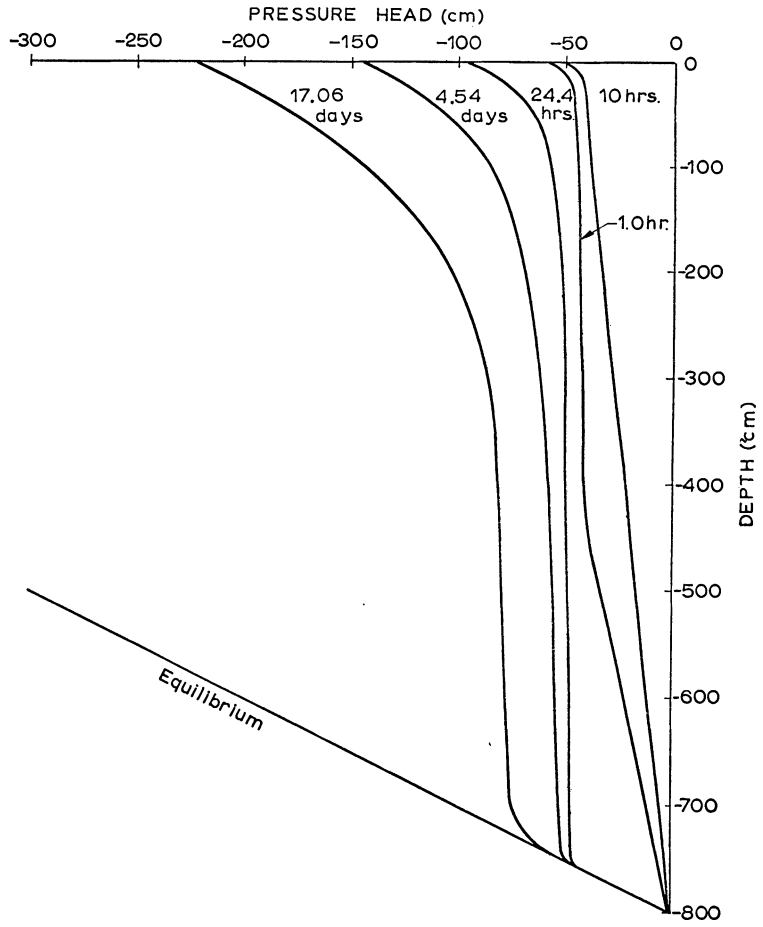


*Fig. 5.*
Pressure head profiles for a 800 cm depth of Botany sand.

The dimensionless outflow form $(Q/Q_\infty)$ is a convenient way of comparing the outflows from different profile depths. Figure 9 gives the outflow for Botany sand for depths of 60, 120, 300, and 800 cm for times up to 1 day. The same information is replotted in Figure 10 with a log time scale so that the longer drainage times can be included. The interesting aspect here is whether it is possible to transform these curves into a fully dimensionless form which will allow them to coalesce so that a general drainage relationship of sufficient accuracy could be determined for Botany sand.

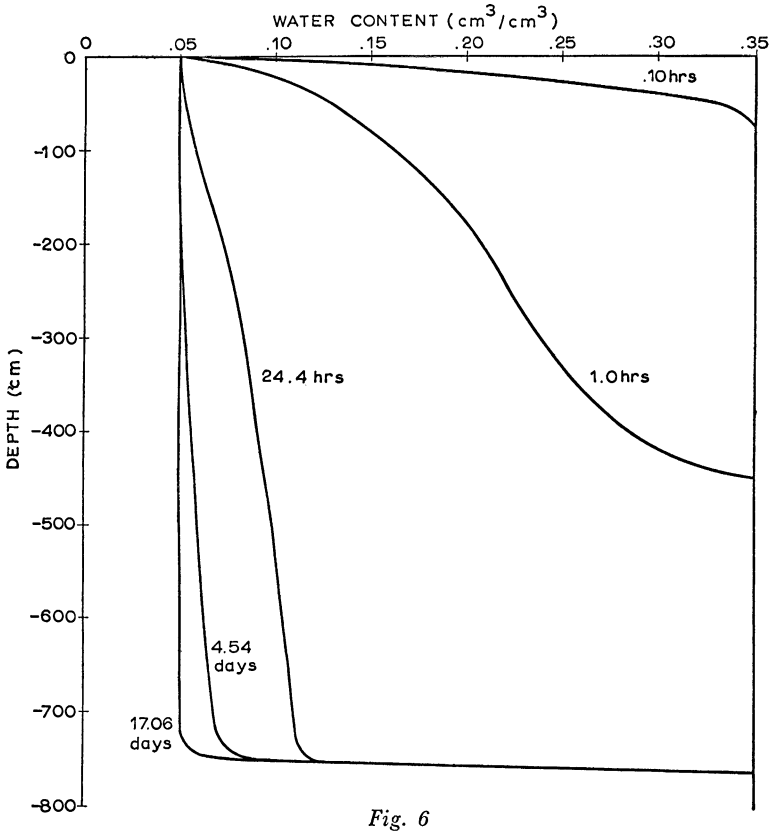


*Fig. 6*

Water content profiles for a 800 cm depth of Botany sand.

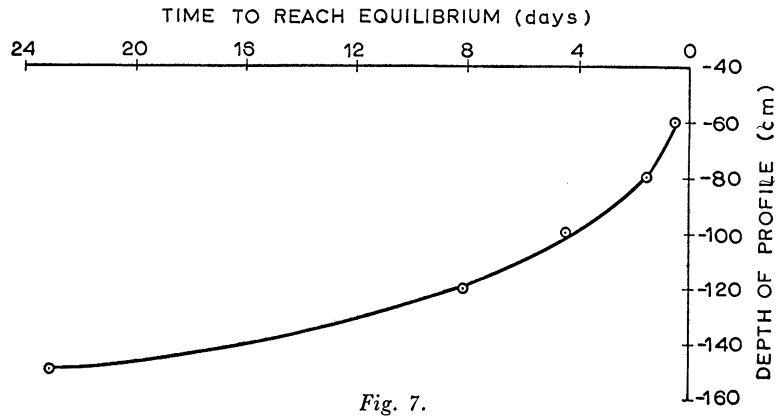


*Fig. 7.*

Time to reach equilibrium for several profile depths.

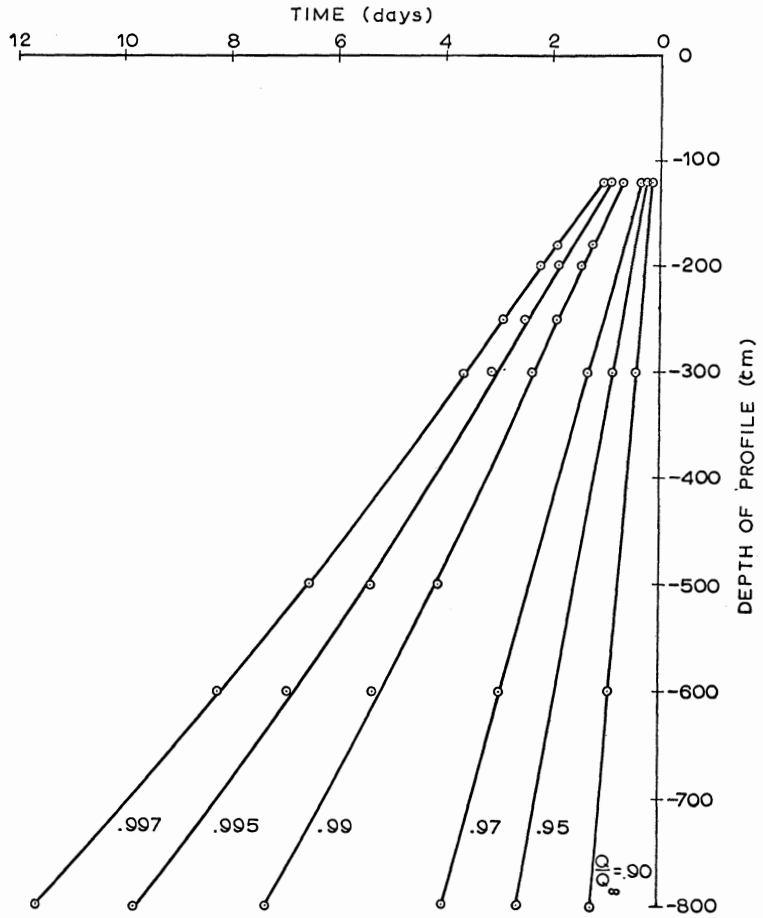


*Fig. 8*
Relationship between time and profile depth for several values of $Q/Q_\infty$

The most convenient dimensionless parameter to use is the parameter $\tau$ introduced by Youngs (1960). It is defined as $q_o t/Q_\infty$ where $q_o$ is the outflow flux at the instant drainage commences and $Q_\infty$ is the total outflow at equilibrium as defined above.

When the data of Figure 10 are changed to this form, the points shown in Figure 11 are obtained. At certain values of $\tau$ the points were so close together that only one could be plotted. If the plotted values for 120, 300, and 800 cm

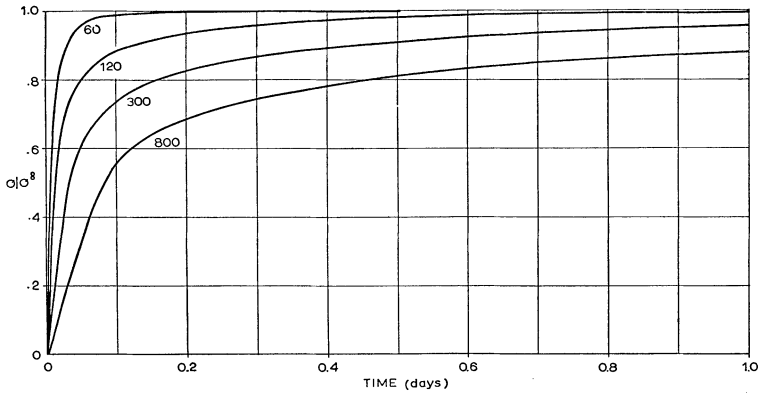


*Fig. 9.*
Relationship between time and $Q/Q_\infty$ for profile depths of 60, 120, 300, and 800 cm.

depth are considered, it is seen that, except in the vicinity of $Q/Q_\infty \equiv 0.40$, the points coalesce to a degree that one curve gives accuracies of 1–2 %. This is quite satisfactory for practical usage. However, as Youngs and others have pointed out, the expression of $Q/Q_\infty \equiv 1\text{–}e^{-\tau}$ poorly represents the $Q/Q_\infty$ relationship. We see therefore that although the use of $\tau$ produces a reasonable single curve, it bears no close relationship to the simple algebraic expression because of the strong nonlinearity of the flow equation. The inclusion of the additional series terms to the above expression results in larger differences be-

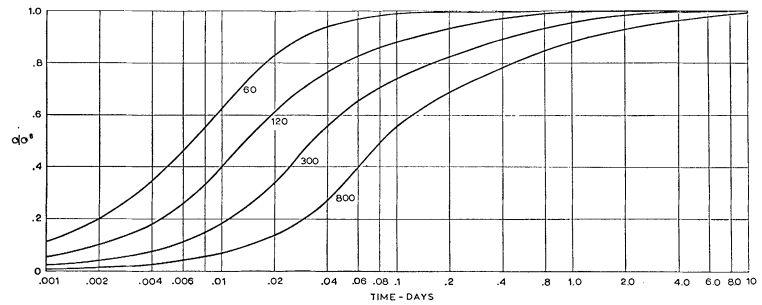


*Fig. 10.*
Relationship between time (log scale) and $Q/Q_\infty$ for profile depths of 60, 120, 300, and 800 cm.

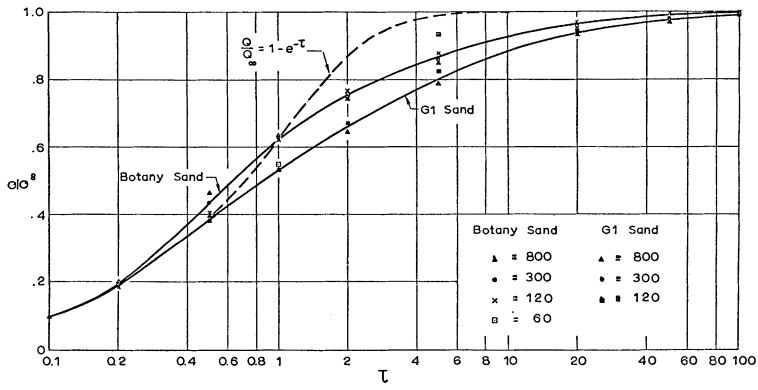


*Fig. 11.*
Dimensionless plot of relationship between $Q/Q_\infty$ and $\tau$ for Botany sand and G1 sand.

tween the curves. It would seem that one computer solution is necessary (say for 300 cm depth) to obtain the form of $Q/Q_\infty \nu \tau$ and then from this the outflow characteristics of all depths are determinable, since $q_o$ and $Q_\infty$ can easily be found as discussed below. Depths of 120, 300, and 800 cm of G1 sand were also analysed and these coalesced even more closely than the Botany sand; however, the relationship is quite distinct from that obtained for Botany sand (see Fig. 11). This reinforces the statement made above, namely that it is always necessary to make one computer solution to position the $Q/Q_\infty \nu \tau$ curve. The points for the 60 cm depth of Botany sand do not lie on the $Q/Q_\infty \nu \tau$ curve and this is to be expected due to the small drainable section. It would seem that the representation of the drainage process by a single curve is limited to depths in excess of three times the air entry value.

A result essentially the same as that of Youngs but developed from a porous model rather than a capillary tube model can be obtained using the approach of Green & Ampt (1911) who specified that water content changes take place at sharply defined fronts. For drainage, this results in one side of the front being at full saturation while the other side is at the very low water content appropriate to long-term drainage. On the $h(\Theta)$ plot the method implies a step function as shown by *BC* in Figure 1 for Botany sand. The position of the line is somewhat arbitrary but the sharp front condition can be clearly visualized from the form of the relationship. Using this $h(\Theta)$ step function, the dimensionless parameter $\tau$ can be rewritten as follows:

Let $L$ be the length (considered positive) of a column of the material of air

entry value $h_A$ and saturated hydraulic conductivity $K_{sat}$. Then $q_o$ the initial flux is given by $K_{sat}\left(\frac{L+h_A}{L}\right)$. This will apply whatever shape the $h(\Theta)$ curve may have but when applied to the step function case, it becomes $K_{sat}\left(\frac{L+h_B}{L}\right)$ where $h_B$ is the pressure head (negative) at B (Fig. 1). $Q_\infty$ can then be written as

$Q_\infty \equiv \Theta_{BC} \times (L+h_B)$ where $\Theta_{BC}$ is the water content difference between saturation at $B$ and the minimum value at $C$.

$$\therefore \tau = \frac{q_o t}{Q_\infty} = \frac{K_{sat}}{\Theta_{BC}} \times \frac{t}{L} = \frac{\alpha t}{L} \tag{30}$$

$$\text{where } \alpha \equiv \frac{K_{sat}}{\Theta_{BC}} \tag{31}$$

Since $\alpha$ is a property of the material regardless of the hydraulic boundary conditions, $t$ can be quickly determined knowing $\tau$ and the length of the column.

Within the accuracy of the approximation, Eq. (30) indicates that for a given $Q/Q_\infty$ value the time to reach that value as given by the curve in Fig.11 is proportional to the length of the column. With very long columns the accuracy of the approximation is good and the substitution of BC for the actual $h(\Theta)$ curve (Figure 1) has little effect on the result; however, with short columns (e. g. 60 cm) the effect is marked and the above approximation cannot be used.

Since $\frac{t}{L}$ is equal to $\frac{\tau}{\alpha}$, a measure of the appropriateness of the approximation should be given by the degree of linearity or otherwise of the plots of $t/L$ for certain $Q/Q_\infty$ values. These have already been plotted in Figure 8 and support the approximation for $Q/Q_\infty$ values of .90, .95, and .97. The departures from linearity for the larger $Q/Q_\infty$ values are not great.

**Drainage of a Stratified Layer**

The drainage of a stratified layer is only briefly discussed here. As previously noted, the solution at this stage is only possible with a coarse-over-fine sequence or sequences. Accordingly, a system consisting of 30 cm of G1 sand over 70 cm of Botany sand was analysed. The pressure condition at zero time is again controlled by the air entry value ($h_A$) of the uppermost layer. However, in this case

it is only one of the controlling factors that produces a profile consisting of two linear sections. To define the profile, the pressure head at the interface ($h_I$) is required. Let $A$ be the top layer with a thickness $L_A$ and hydraulic conductivity at saturation of $K_A$ and $B$ the lower layer of thickness $L_B$ and conductivity $K_B$.

Then

$$h_I = \frac{h_A L_B K_A + L_A L_B (K_A - K_B)}{L_A K_B + L_B K_A} \tag{32}$$

$L_A$ and $L_B$ are positive in Eq. (32) and $h_A$ assumes its characteristic negative sign on numerical substitution.

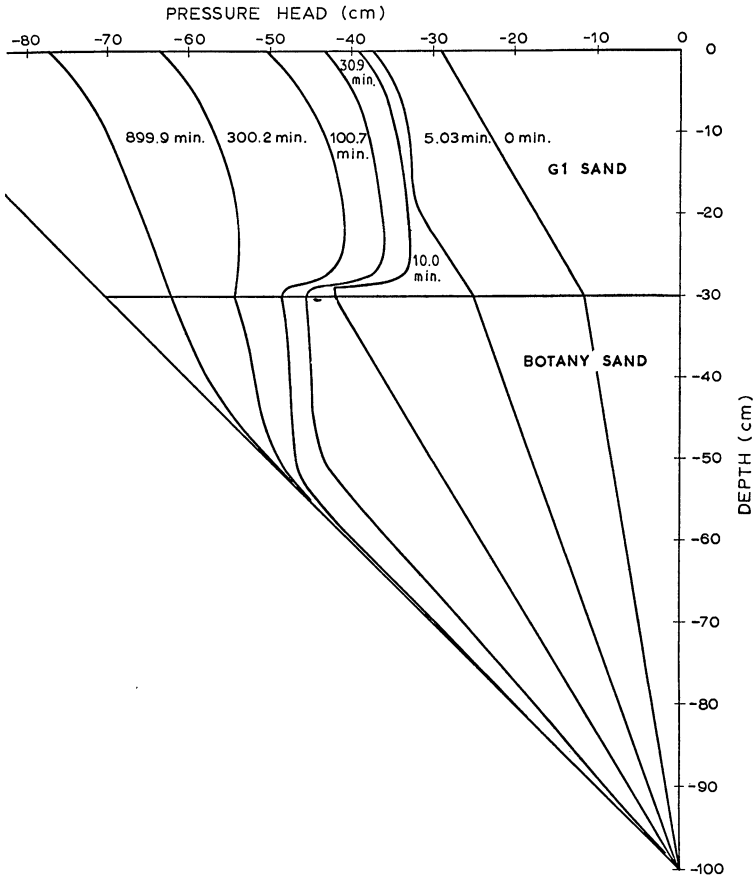


*Fig. 12.*
Pressure head profiles for a stratified horizon consisting of 30 cm of G1 sand over 70 cm of Botany sand.

Figures 12 and 13 give $h(z, t)$ and $\Theta(z, t)$ for the stratified case described above.

**Ponded Infiltration into a Draining Profile**

This system is illustrated numerically by considering a 400 cm depth of Botany sand which is draining to a water table. The initial conditions for the infiltration phase are the pressure head profiles at times of 31.1 minutes and 1.04 days after

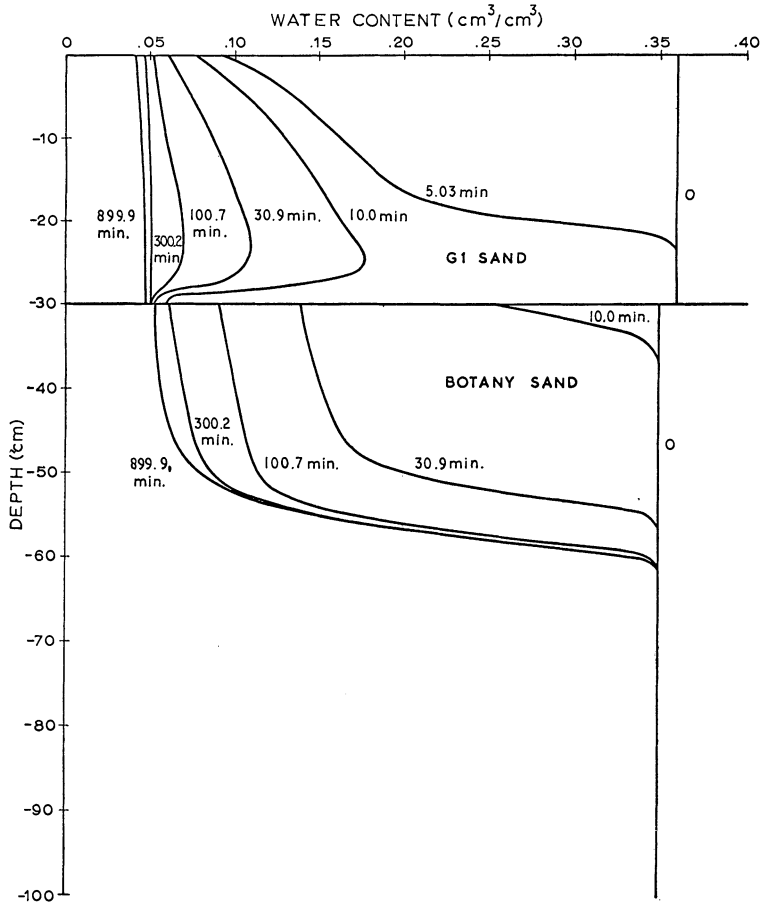


*Fig. 13.*
Water content profiles for a stratified horizon consisting of 30 cm of G1 sand over 70 cm of Botany sand.

the start of the drainage. The depth of water on the surface is 15 cm. The pressure head profiles after 25.2 min of wetting are given in Figure 14. The continuing drainage of the 31.1 min initial profile is clearly seen during the wetting

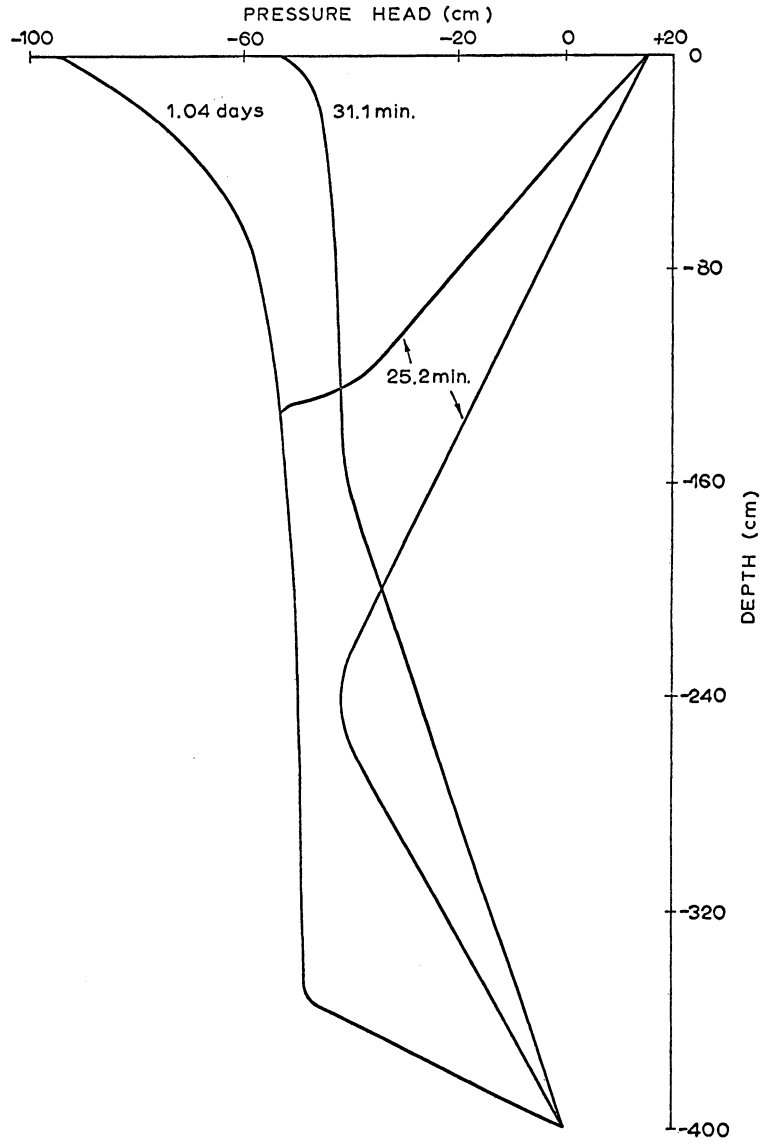


*Fig. 14.*
Pressure head profiles for 25.2 minutes of infiltration into two columns allowed to drain for 31.1 minutes and 1.04 days.

up period in contrast to the 1.04 day initial profile where the drainage is negligible over 25.2 minutes. The system is discussed in detail by Whisler & Watson (1969).

## LABORATORY INSTRUMENTATION

In this paper laboratory studies being carried out to test computer-predicted pressure head and water content profiles will not be discussed. However, a brief description of some newly acquired equipment which is now in use seems appropriate. Watson (1965) has described rapid response equipment for non-destructive measurement of water content and pressure head using gamma-ray attenuation techniques and a tensiometer-pressure transducer system.

The main disadvantage in the equipment lies in the time required to switch from one hydraulic lead to another when up to twenty tensiometers are in use. In the more recently developed instrumentation sufficient miniature pressure transducers have been purchased to mount one with each tensiometer. These transducers are automatically scanned using a digital voltmeter and scanner at a maximum rate of 10 channels per second, thus giving an almost instantaneous pressure head profile. Such an arrangement allows very rapid pressure changes to be monitored and, in addition, is suitable for measurements at the drier end of the $h(\Theta)$ curve for sands. These measurements were not possible with the hydraulic switching arrangement. The equipment has been designed for use with two-dimensional as well as one-dimensional models and is ideal for this purpose.

The nucleonic equipment has also been updated with the purchase of higher stability modular units. This equipment is particularly necessary for long term experiments. In past experimentation the radioisotope $^{137}Cs$, which has an energy of 0.66 MeV and a half-life of 30 years, has been used. However, there are certain advantages in using a low energy gamma source and for this purpose a 200 mCi source of $^{241}Am$, which has an energy of 0.06 MeV and a half-life of 458 years, has been purchased. The availability of both sources also allows the method to be used with swelling soils. This is achieved by taking gamma counts with each source and solving the attenuation equations simultaneously.

The output from the scanning system is at present being fed into a high speed paper tape unit. This is necessary for control purposes during the running of an experiment. However, it is intended to extend the system with an incremental tape deck so that the experimental data can be read directly into the IBM 360/50 computer for analysis.

## ACKNOWLEDGMENTS

The support of the Australian Research Grants Committee in providing funds for the purchase of equipment and for computer time is warmly acknowledged.

## REFERENCES

Green, W. H. & Ampt, S. A. (1911) Studies in soil physics, 1. The flow of air and water through soils. *J. Agr. Sci. 4,* 1–24.

Jensen, M. E. & Hanks, R. J. (1967) Nonsteady-state drainage from porous media. *J. Irrig. and Drainage Div., ASCE,* 93, IR3, 209–231.

Liakopoulos, A. C. (1964) Theoretical solution of the gravity drainage problem. *J. Hydraulic. Res. 2,* 50–74.

Philip, J. R. (1969) Theory of infiltration. *Advances in Hydroscience 5,* 216–296.

Sedgley, R. H. (1967) Water content – pressure head relationships in a porous medium. Unpublished Ph. D. Thesis, University of Illinois.

Watson, K. K. (1965) The measurement of non-continuous unsteady flow in long soil columns. *Moisture Equilibria and Moisture Changes in Soils beneath Covered Areas.* Butterworth, Sydney, pp 70–77.

Watson, K. K. (1967) Numerical and experimental study of column drainage. *J. Hydraulics Div. ASCE,* 93, HY2, 1–15.

Whisler, F. D. & Watson, K. K. (1968) One-dimensional gravity drainage of uniform columns of porous materials. *J. Hydrology 6,* 277–296.

Whisler, F. D. & Watson, K. K. (1969) Analysis of infiltration into draining porous media. *J. Irrig. and Drainage Div., ASCE,* 95, IR4, 481–491.

Youngs, E. G. (1960) The drainage of liquids from porous materials. *J. Geophys. Res. 65,* 4025–4030.

*Address:*
Dr. K. K. Watson,
Associate Professor of Civil Engineering, The University of New South Wales,
Box 1, Post Office, Kensington, New South Wales, Australia.

Received 17 February 1970.